Programmable polyproteams built using twin peptide superglues

Gianluca Veggiani[a], Tomohiko Nakamura[a,b], Michael D. Brenner[a], Raphaël V. Gayet[a,c], Jun Yan[d], Carol V. Robinson[d], and Mark Howarth[a,1]

[a]Department of Biochemistry, University of Oxford, Oxford, OX1 3QU, United Kingdom; [b]LOC Development Department, R&D Division, Medical Business Unit, Sony Corporation, 1-5-45 Yushima, Bunkyo-ku, Tokyo 113-8510, Japan; [c]Ecole Normale Supérieure de Lyon, 69364 Lyon Cedex 07, France; and [d]Department of Chemistry, Physical and Theoretical Chemistry Laboratory, University of Oxford, Oxford, OX1 3QZ, United Kingdom

Edited by Samuel H. Gellman, University of Wisconsin–Madison, Madison, WI, and approved December 24, 2015 (received for review September 28, 2015)

Programmed connection of amino acids or nucleotides into chains introduced a revolution in control of biological function. Reacting proteins together is more complex because of the number of reactive groups and delicate stability. Here we achieved sequence-programmed irreversible connection of protein units, forming polyprotein teams by sequential amidation and transamidation. SpyTag peptide is engineered to spontaneously form an isopeptide bond with SpyCatcher protein. By engineering the adhesin RrgA from *Streptococcus pneumoniae*, we developed the peptide SnoopTag, which formed a spontaneous isopeptide bond to its protein partner SnoopCatcher with >99% yield and no cross-reaction to SpyTag/SpyCatcher. Solid-phase attachment followed by sequential SpyTag or SnoopTag reaction between building-blocks enabled iterative extension. Linear, branched, and combinatorial polyproteins were synthesized, identifying optimal combinations of ligands against death receptors and growth factor receptors for cancer cell death signal activation. This simple and modular route to programmable "polyproteams" should enable exploration of a new area of biological space.

synthetic biology | protein engineering | nanobiotechnology | split protein | antibody

Biological events usually depend on the cooperative activity of multiple proteins. Clustering a single kind of protein often greatly enhances biological signals (1), for example in the repeating antigen structures on vaccines (2). However, clustering different kinds of proteins into programmed polyprotein teams ("polyproteams") is an unmet challenge (3, 4). Protein units can be joined genetically into one long open reading frame, but errors in protein synthesis and misfolding soon become limiting (5, 6). Expressing modules individually and then linking the modules together would overcome these challenges as well as allow independent posttranslational modification of each module. Even the best noncovalent linkages (7–9) or reversible covalent linkages, including disulfide bonds (10, 11), would allow rearrangement of polyproteams, so irreversible covalent linkage is required. There are a limited number of mutually unreactive (orthogonal) chemical reactions (12); therefore, it is impractical to link more than a few building blocks in a one-pot reaction. However, elongating one step at a time allows chain growth using a small number of orthogonal connections (13). If the growing chain is attached to a solid phase, the reacting module can be added in large excess (driving reaction to completion), with unreacted building blocks simply washed away (so separation is unnecessary at each step). Establishing such solid-phase chemistry for connecting amino acids underpinned the breakthroughs in the biological understanding and therapeutic use of peptides (14, 15), whereas the solid-phase synthesis of DNA primers underpinned the revolution in gene amplification and reengineering (16, 17). Solid-phase reaction has also enabled the ligation of peptide fragments to make synthetic proteins (18, 19).

Other important features of a system for synthesizing polyproteams are molecularly defined connections, independence from any template (20, 21), and simple expression of each module. Nearly quantitative yield for each reaction is required; otherwise, after a few steps the incomplete chains generate hopelessly heterogeneous products. In addition, it is preferable for modules to be modified with peptide tags rather than protein fusion domains (e.g., HaloTag or SNAP-tag) for minimal disruption to module function (22, 23). For unbreakable linkage to a peptide, we previously developed the use of spontaneous isopeptide bond formation (24, 25). SpyTag is a 13-amino-acid peptide that can be genetically fused to the protein of interest, and upon mixing with its protein partner SpyCatcher, an Asp of SpyTag forms a spontaneous isopeptide bond with a Lys of SpyCatcher (26). Reaction occurs with good specificity (27) and under a wide range of conditions, with a connection resistant to boiling in SDS and high force (26).

To enable synthesis of polyproteams, here we first developed a covalent peptide/protein pair (SnoopTag/SnoopCatcher) orthogonal to SpyTag/SpyCatcher. Using iterative Snoop and Spy reactions, we then established the synthesis of linear and branched polyproteams. Polyproteams were analyzed by electrophoresis, chromatography, and mass spectrometry. We then synthesized combinations of polyproteins for sensitive activation of cancer cell death.

Significance

Many biological events depend on proteins working together as a team. Here we establish how to program team formation, covalently linking protein modules step by step. We split a domain from *Streptococcus pneumoniae* to form a peptide and protein pair, SnoopTag and SnoopCatcher, which form an isopeptide bond when mixed together. SnoopTag/SnoopCatcher reacted with each other but not with an alternative peptide/protein pair, SpyTag/SpyCatcher. We formed polyprotein chains by alternating SpyTag reaction with SnoopTag reaction. Cellular signaling often relies on integrated activation of different receptors, so we built polyprotein teams to stimulate Death Receptor and Growth Factor receptors, finding an optimal combination for cell-death induction in cancer cells. Programmable "polyproteams" provide a simple route to investigate or harness biological teamwork.

Author contributions: G.V., T.N., R.V.G., J.Y., and M.H. designed research; G.V., T.N., M.D.B., and J.Y. performed research; R.V.G. contributed new reagents/analytic tools; G.V., T.N., M.D.B., J.Y., C.V.R., and M.H. analyzed data; and G.V. and M.H. wrote the paper.

Conflict of interest statement: M.H. is an inventor on patent EP2534484, which applies to spontaneous isopeptide bond formation to a peptide tag, and United Kingdom Patent Application No. 1509782.7, which applies to iterative synthesis through isopeptide bonds.

This article is a PNAS Direct Submission.

Data deposition: The sequences reported in this paper have been deposited in the GenBank database (accession nos. KU296973, KU296974, KU296975, KU296976, KU356870, KU361182, KU361183, KU500643, KU500644, KU500645, and KU500646).

[1]To whom correspondence should be addressed. Email: mark.howarth@bioch.ox.ac.uk.

This article contains supporting information online at www.pnas.org/lookup/suppl/doi:10.1073/pnas.1519214113/-/DCSupplemental.

Results

Design of an Orthogonal Covalent Peptide–Protein Interaction. RrgA is an adhesin from *Streptococcus pneumoniae*, a Gram-positive bacterium that can cause septicemia, pneumonia, and meningitis in humans. A spontaneous isopeptide bond forms in the D4 Ig-like domain of RrgA between residues Lys742 and Asn854 (Fig. 1*A*) (28). We split the D4 domain in the loop following the N-terminal β-strand and, after exploring various extensions and truncations of the two partners, settled on the peptide tag we termed SnoopTag (residues 734–745) and the protein partner we named SnoopCatcher (residues 749–860; Fig. 1*B*). To optimize reaction, SnoopCatcher included the mutations G842T, designed to stabilize a β-strand, and D848G, designed to stabilize a hairpin turn close to the reaction site (Fig. S1*A*). SnoopTag fused to maltose-binding protein (MBP) and SnoopCatcher were expressed efficiently as soluble proteins in the cytosol of *Escherichia coli* and purified by nickel-nitrilotriacetic acid (Ni-NTA) affinity chromatography. SnoopTag-MBP and SnoopCatcher, simply upon mixing, formed a complex stable to boiling in SDS (Fig. 1*C*). Mutations in the putative reactive Lys742 of SnoopTag (SnoopTag KA-MBP) and the putative reactive Asn854 of SnoopCatcher (SnoopCatcher NA) abolished reaction (Fig. 1*C*). Electrospray ionization mass spectrometry was consistent with the loss of NH_3 resulting from isopeptide bond formation between SnoopCatcher and SnoopTag; acetylated and gluconylated side products common for *E. coli* overexpression were also observed (Fig. 1*D*). With a 1:1 SnoopCatcher to SnoopTag-MBP,

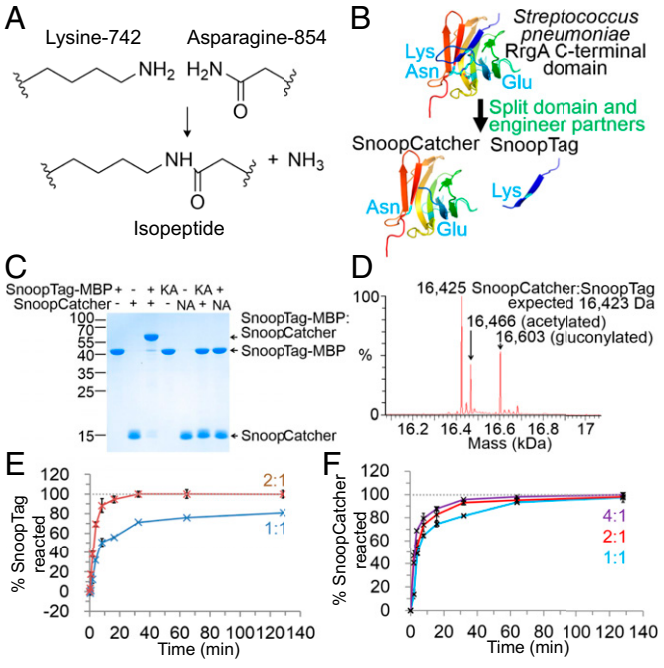

Fig. 1. Establishing the covalently reactive peptide/protein pair SnoopTag and SnoopCatcher. (*A*) Spontaneous isopeptide bond formation between Lys and Asn, releasing ammonia. (*B*) Cartoon of splitting RrgA D4 domain [based on Protein Data Bank (PDB) ID code 2WW8] to make SnoopTag and SnoopCatcher. Reactive residues are in cyan. (*C*) SnoopTag-MBP reaction with SnoopCatcher, each at 10 μM, after 2 h at 25 °C analyzed by SDS/PAGE with Coomassie staining, alongside controls with Ala mutation of SnoopTag's reactive Lys (KA) or SnoopCatcher's reactive Asn (NA). (*D*) Isopeptide bond formation between SnoopTag peptide and SnoopCatcher shown by mass spectrometry. (*E*) Time course of SnoopTag reaction with a 1:1 or 2:1 ratio of SnoopCatcher to SnoopTag-MBP, tested as in *C*. (*F*) Time course of SnoopCatcher reaction with a 1:1, 2:1, or 4:1 ratio of SnoopTag-MBP to SnoopCatcher, tested as in *C*. Error bars are mean ±1 SD; $n = 3$. Some error bars are too small to be visible.

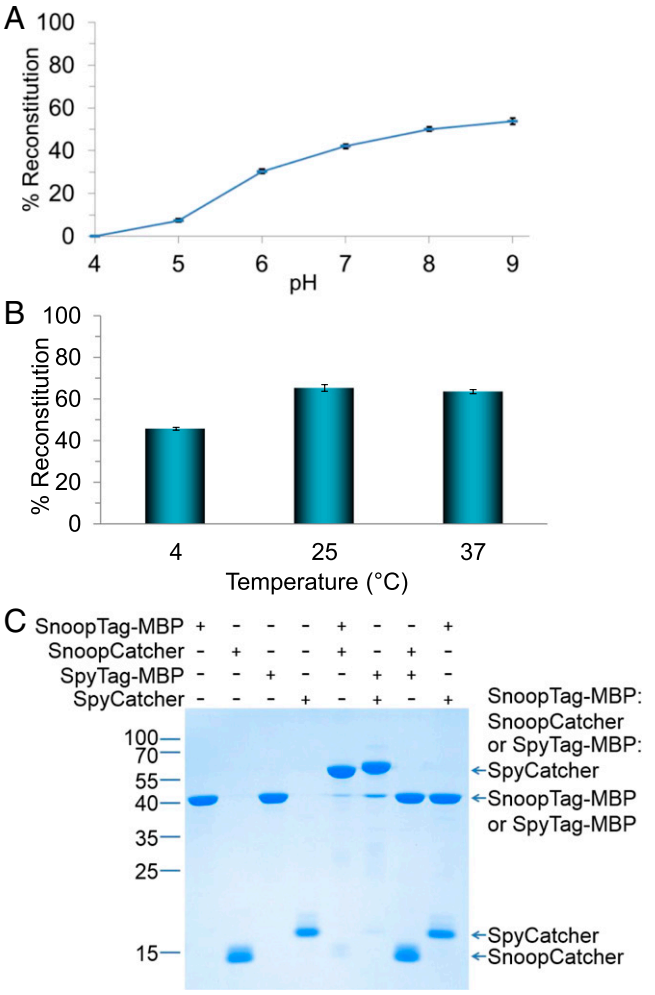

Fig. 2. SnoopTag reaction is robust to conditions and orthogonal to SpyTag. (*A*) For pH dependence, 10 μM SnoopTag-MBP was incubated with 10 μM SnoopCatcher at the indicated pH for 15 min at 25 °C and analyzed by SDS/PAGE with Coomassie staining. (*B*) Temperature dependence of SnoopTag/SnoopCatcher reaction tested as in *A*. (*C*) SnoopTag/SnoopCatcher and SpyTag/SpyCatcher orthogonal reactivity, after incubation for 18 h at 25 °C, with each species at 10 μM, determined by SDS/PAGE with Coomassie staining. Error bars are all mean ± 1 SD; $n = 3$. Some error bars are too small to be visible.

~80% of SnoopTag-MBP reacted. However, with a twofold excess of SnoopCatcher, SnoopTag-MBP reacted quantitatively (Fig. 1*E* and Fig. S1*B*). Similarly with an excess of SnoopTag-MBP, SnoopCatcher was ~100% consumed (Fig. 1*F* and Fig. S1*C*). We established that reaction proceeded efficiently from pH 6–9 (Fig. 2*A*) and 4–37 °C (Fig. 2*B*). Cysteine is absent from SnoopTag and SnoopCatcher, so, as expected, the reaction was insensitive to DTT (Fig. S1*D*). No specific buffer component was required, with reaction in PBS as well as in the presence of the detergents Triton X-100 and Tween-20, or high salt (1 M NaCl) (Fig. S1*D*). The chemical chaperone trimethylamine *N*-oxide (TMAO) (29) modestly enhanced reaction (Fig. S1*E*).

Spontaneous hydrolysis of an amide bond normally takes years under neutral conditions (30), but we tested if hydrolysis was accelerated in this protein environment. We looked for reversal of the SnoopTag-MBP/SnoopCatcher interaction, by competing with excess of an alternative SnoopTag-linked protein or ammonia, but we did not observe reversibility (Fig. S2).

SnoopTag has a reactive Lys (Fig. 1*B*), whereas SpyTag has a reactive Asp (26), so we hypothesized that SnoopTag/SnoopCatcher

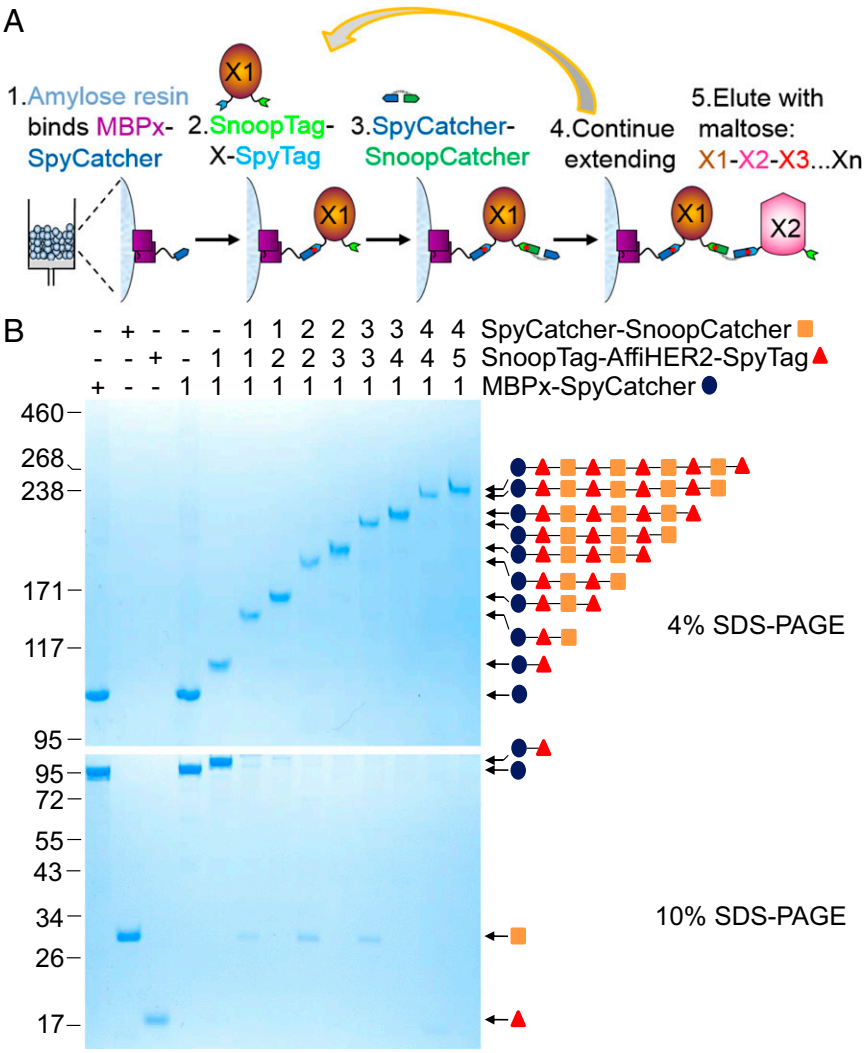

Fig. 3. Solid-phase polyproteam synthesis. (*A*) Principle of polyproteam synthesis. Amylose resin is bound by modified MBP linked to SpyCatcher (MBPx-SpyCatcher). A protein of interest bearing SpyTag and SnoopTag is added to the resin and reacts with SpyCatcher on the growing chain (red line represents an isopeptide bond). SpyCatcher–SnoopCatcher is added and reacts with SnoopTag of the growing chain. Extension is continued by sequential additions of SnoopTag–X–SpyTag and SpyCatcher–SnoopCatcher. After extension is completed, the polyproteam is eluted from the resin with maltose. (*B*) Analysis of solid-phase polyproteam synthesis. Lanes 1–3 show MBPx-SpyCatcher, SpyCatcher–SnoopCatcher, and SnoopTag–AffiHER2–SpyTag in isolation. MBPx-SpyCatcher was bound to the amylose resin, and stepwise reaction with SnoopTag–AffiHER2–SpyTag and SpyCatcher–SnoopCatcher was carried out. After each stage, one aliquot of sample was eluted from the resin with maltose (lanes 4–13). Samples, without further purification, were analyzed by SDS/PAGE [both 4% and 10% (wt/vol) gels] with Coomassie staining.

and SpyTag/SpyCatcher pairs would be fully orthogonal. Each partner reacted efficiently with its cognate pair, but we found no trace of cross-reaction, even after overnight incubation (Fig. 2*C*). SpyTag and SpyCatcher also reacted to more than >95% conversion with an excess of their cognate partner (Fig. S3). Therefore, SnoopTag/SnoopCatcher provides a robust system for irreversible protein linkage and can be used in partnership with SpyTag/SpyCatcher.

Establishment of Solid-Phase Polyproteam Synthesis. Having dual orthogonal covalent reactions, we set out to achieve solid-phase iterative synthesis of polyproteins (Fig. 3*A*). The interaction of *E. coli* MBP with amylose resin is widely used in affinity purification: MBP fusions typically express well, with low nonspecific resin binding and selective mild elution using maltose. The affinity of wild-type MBP for maltose is 1.2 μM (31), which is satisfactory for protein purification but insufficient for multiple rounds of washing and chain extension in polyproteam synthesis. Therefore, we combined mutations enhancing MBP's maltose-binding stability (A312V, I317V, and deletion at 172, 173, 175, and 176) (Fig. S4*A*) (31, 32). We then tandemly linked this MBP mutant to generate MBPx-SpyCatcher (His_6–MBPmt–linker–MBPmt–SpyCatcher) for anchoring to amylose. For initial chain building, we incorporated affibodies, nonimmunoglobulin scaffolds expressed efficiently in *E. coli*. The affibody to the receptor tyrosine kinase and proto-oncogene HER2 (human epidermal growth factor receptor 2) (33) was linked at its N terminus with SnoopTag and at its C terminus with SpyTag (SnoopTag–AffiHER2–SpyTag). Affibody units were bridged using SpyCatcher connected through a helical spacer to SnoopCatcher (SpyCatcher–SnoopCatcher also expressed efficiently as a soluble protein in *E. coli*) (Fig. 3*A*). Because each linkage is covalent, chain synthesis could be easily followed by adding maltose to elute from the resin and then SDS/PAGE (Fig. 3*B*). MBPx-SpyCatcher reacted quantitatively with SnoopTag–AffiHER2–SpyTag (Fig. 3*B*, lane 5). This construct then reacted quantitatively with SpyCatcher–SnoopCatcher (Fig. 3*B*, lane 6). Sequential addition of SnoopTag–AffiHER2–SpyTag and SpyCatcher–SnoopCatcher enabled chain growth with high purity, extending to a product 10 units long (a decamer; Fig. 3*B*, lane 13). To demonstrate solid-phase extension with a different solid phase, we used biotin–SpyCatcher linked to monomeric avidin beads: Polyproteams were assembled to a decamer and eluted with free biotin (Fig. S4*B*).

Analysis of the Decamer Polyproteam. Because chain units are connected via internal isopeptide bonds, the SDS/PAGE mobility of the chain diverges from the predicted molecular weight. To validate the identity of the assembled decamer, we initially performed electrospray ionization mass spectrometry, showing good correspondence between observed mass (285 kDa with a SD of 3 kDa) and expected mass (282.5 kDa) (Fig. 4*A*). Size-exclusion

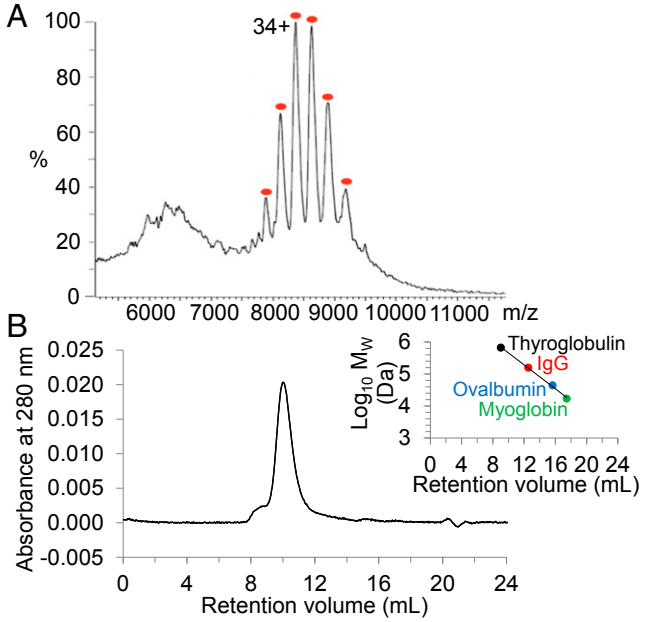

Fig. 4. Biophysical analysis of polyproteams. (*A*) Electrospray ionization mass spectrometry to test identity of decamer polyproteam, MBPx-SpyCatcher:(SnoopTag–AffiHER2–SpyTag:SpyCatcher–SnoopCatcher)$_4$:SnoopTag–AffiHER2–SpyTag. Red circles correspond to the decamer, with the charge state of the highest peak marked. (*B*) Size-exclusion chromatography of the same polyproteam. The *Inset* shows the molecular weight standards.

chromatography of the decamer showed one major peak centered at ∼287 kDa, based on calibration with protein standards, consistent with the expected monomeric mass and indicating that there was minimal self-association under these conditions (Fig. 4*B*). To assess thermostability, the decamer was heated at a range of temperatures and centrifuged to remove aggregates: the decamer remained largely soluble even at 70 °C (Fig. S5*A*). We also tested decamer integrity to storage: after 1 or 4 d at 25 °C, we saw little degradation and little loss of solubility (Fig. S5*B*).

Expanding from the initial incorporation of AffiHER2 modules into chains, we generated fluorescent protein polyproteams (Fig. S6*A*). We also generated bottle-brush polyproteams by joining a tandemly linked affibody against HER2, where both the tags were at the N terminus (SnoopTag–SpyTag–AffiHER2 × 3), so that the binding units branched from a central core (Fig. S6*B*) (34).

Application of Polyproteins to Combinatorial Cell Signaling. We established combinatorial synthesis of polyproteams using a simple 96-well plate format. These polyproteams were used to probe the spatial integration between different signaling pathways. Cancer cells are frequently sensitized to cell death induced by Death Receptor signaling, but clinical results have been disappointing using bivalent IgG, which is not potent at cell death induction (35, 36). We set out to explore higher multivalency and how Death Receptor signaling interacts with signaling by growth factor receptors frequently overexpressed in cancer. Therefore, we created combinations of polyproteams with repeats of a nanobody agonist for Death Receptor 5 (DR5) and an affibody to either epidermal growth factor receptor (EGFR), HER2, or type I insulin-like growth factor receptor (IGF1R) (Fig. 5). These proapoptotic polyproteams were synthesized with good purity (Fig. 5*A*). Each of the combinatorial polyproteams bearing four nanobodies and one affibody unit at each of five positions was tested for effects on viability of the breast cancer cell line MDA-MB-231. Affibody position affected cytotoxicity, with optimal killing by the chain with four nanobodies (N) followed by an affibody to EGFR (E) (NNNNE chain; Fig. 5*B*). Negative-control polyproteams containing only affibodies to HER2 (HHHHH), EGFR (EEEEE), IGF1R (IIIII), or Taq polymerase (i.e., a ligand not present on the cell surface) (TTTTT) showed no toxicity (Fig. S7). We further assessed the dose dependence of NNNNE cytotoxicity (Fig. 5*C*). Most of the cytotoxicity of NNNNE was apparent at 24 h (Fig. 5*D*). NNNNE induced potent activation of caspase signaling, similarly to tumor necrosis factor-related apoptosis-inducing ligand (TRAIL, the endogenous DR5 agonist), and NNNNE's effect was fully blocked by the caspase inhibitor Benzyloxycarbonyl–Val-Ala-Asp–fluoromethylketone (Z-VAD-FMK). HHHHH did not activate caspases (Fig. 5*E*).

To test the role of valency in polyproteam activation of cell death, we synthesized decamers having varying numbers of anti-DR5 nanobodies alongside either affibodies to EGFR or negative-control affibodies to Taq polymerase (Fig. S7). Polyproteams with one or two nanobodies did not induce cell death, but killing gradually increased as the nanobody valency increased from three to five. With three or four nanobodies in the chain, compared with the anti-Taq control, targeting to EGFR enhanced the polyproteam potency (Fig. S7*B*).

Discussion

We have generated a modular approach to synthesis of programmed polyproteams, through spontaneous isopeptide bond formation between peptide tags. The polyproteams are linked through irreversible amide bonds and so are stable over time (if protected from proteases) and allow easy analysis by SDS/PAGE. The initiation, extension, and release steps use mild conditions, independent of redox state, and therefore should be applicable to a wide range of proteins. With only a single way for the chain to grow, products are molecularly defined, favoring reproducibility and precise tuning of function. Also, subunits do not need to be connected in an *N* to C orientation, as we show with bottle-brush polymer architectures. No chemical modification of the module is required, avoiding time-consuming and hard-to-control bioconjugation steps, so our method is accessible to any laboratory able to express recombinant proteins. Combinatorial synthesis of polyproteams allows rapid testing of patterns able to give potent cellular signal activation.

Spontaneous isopeptide bond formation has the advantage of a simple reaction pathway between two functional groups having low intrinsic reactivity (an amine with a carboxylic acid or a carboxamide), so there is little side reaction (26, 37) and yields for each step were almost quantitative (38). This enabled a high purity of polyproteams after nine consecutive reactions. Polyproteam assembly is not traceless, leaving a SpyCatcher–SnoopCatcher unit between each module. In future work, it will be interesting to explore SpyCatcher–SnoopCatcher units with alternative sizes and orientations, as well as using other linkage chemistries for solid-phase synthesis. Sortase, subtiligase, transglutaminase, and split inteins enable covalent protein–protein interaction that is either traceless or leaves a short peptide tag (39–43), and these approaches will be valuable to test in the future with MBPx attachment and maltose elution. However, those reactions pass through a (thio)ester intermediate, so hydrolysis may compete with ligation (39, 40). Artificial amino acids for bioorthogonal reaction would enable minimal modification but with some issues: the increased complexity of module expression and competing reactions [such as azide reduction (44), alkyne reaction with thiols (45), and spontaneous tetrazine degradation (46)] as well as competition from suppression of stop codons by normal amino acids (47). Recent work demonstrated the synthesis of ubiquitin homo-polymers by azide–alkyne (48), thiol-ene (49), or native chemical ligation reactions (50). A potential disadvantage of our approach is that Tag/Catchers are not human and therefore are likely to be immunogenic, although nonhuman connectors are advantageous for vaccination. Also, each module must have a single SpyTag and SnoopTag, which is straightforward for monomers or

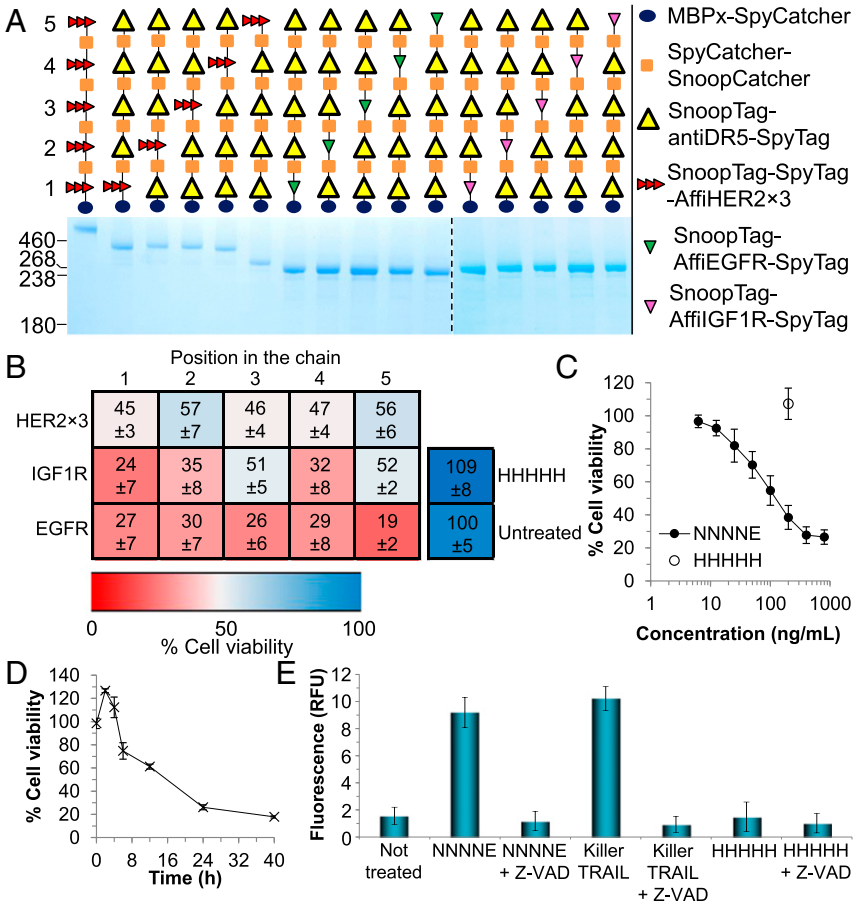

Fig. 5. Combinatorial synthesis of polyproteams. (*A*) Chain synthesis with four anti-DR5 nanobodies and one affibody-based unit at various positions, analyzed by SDS/PAGE with Coomassie staining. (*B*) Polyprotein effect on viability of MDA–MB-231 cells after 40 h of incubation with each chain from *A* at 200 ng/mL, shown as a heat-map. (*C*) Viability of MDA–MB-231 cells at 40 h with titration of NNNNE and HHHHH control (N, anti-DR5 nanobody; E, AffiEGFR; H, AffiHER2 × 3). (*D*) Time course of cytotoxicity with 200 ng/mL NNNNE on MDA–MB-231 cells. (*E*) Caspase reporter activation in response to NNNNE, KillerTRAIL (a DR5 agonist) or HHHHH with or without Z-VAD-FMK pan-caspase inhibitor. (Error bars in each case are mean ± 1 SD; $n = 3$. Some error bars are too small to be visible.)

heteromultimers but needs careful attention for homo-multimers. As one makes larger polyproteams, their solubility and colloidal characteristics will change, just as multidomain extracellular matrix proteins such as fibronectin cannot be treated in the same way as small globular proteins. However, the affibody polyproteam showed good stability over time and to heating. Polyproteams should be a powerful platform to dissect the spatial requirements for cellular signaling, such as in immunity and differentiation (51–53). Other applications of this simple route to new biological architectures may include vaccination (2), biomaterials (34, 54–56), multienzyme organization (9), and enhancing capture of circulating tumor cells (57).

Materials and Methods

Isopeptide Bond Reconstitution Reactions. *SI Materials and Methods* provides a full description of cloning, protein expression and purification, MS, size-exclusion chromatography, cell culture, stability testing of chains, combinatorial assembly of chains, and caspase activation assay. To assess the formation of a covalent bond between SnoopTag and SnoopCatcher, proteins were mixed each at 10 μM final concentration in Tris-buffered saline (TBS) pH 8.0 containing 1.5 M TMAO (Sigma-Aldrich). Reactions were stopped by adding 6× SDS loading buffer [0.23 M Tris·HCl, pH 6.8, 24% (vol/vol) glycerol, 120 μM bromophenol blue, 0.23 M SDS]. Samples were subsequently heated using a Bio-Rad C1000 thermal cycler at 95 °C for 5 min, before SDS/PAGE on 16% (wt/vol) polyacrylamide gels using an XCell SureLock gel container (Life Technologies) at 200 V. SDS/PAGE running buffer was Tris–glycine, except Tris–acetate buffer was used to improve resolution of high-molecular-weight products, as described previously (7). Gels were stained with InstantBlue Coomassie stain (Triple Red Ltd.), and bands were densitometrically analyzed using a Gel Doc XR imager and Image Lab 3.0 software (Bio-Rad).

Solid-Phase Synthesis of Chains. We applied 40 μL slurry amylose resin (New England BioLabs) to a 1 mL poly-prep column (Bio-Rad), rinsed the resin with 1 mL MilliQ water, and equilibrated the resin with 1 mL TBS pH 8.0. We added 320 pmol MBPx-SpyCatcher in TBS pH 8.0 in a final volume of 80 μL to the resin and incubated the resin at 25 °C for 1 h with 700 rpm shaking on a ThermoMixer comfort (Eppendorf). Unreacted protein was removed by gravity flow, and resin was washed with 1 mL wash buffer (50 mM Tris·HCl pH 8.0 with 500 mM NaCl). We added 3 nmol monomer containing a SnoopTag and a SpyTag in TBS pH 8.0 in a final volume of 80 μL to the resin and incubated the resin at 25 °C for 1 h with 700 rpm shaking. Unreacted SnoopTag/SpyTag monomer was removed from the column by gravity flow and resin washed with 1 mL wash buffer. We added 4 nmol SpyCatcher–SnoopCatcher in TBS pH 8.0 with 1.5 M TMAO to the resin and incubated the resin at 25 °C for 2 h with 700 rpm shaking. Unreacted SpyCatcher–SnoopCatcher was removed by gravity flow, and resin was washed with 1 mL wash buffer. Chains were produced by sequential addition of SnoopTag/SpyTag monomer and SpyCatcher-SnoopCatcher, according to the conditions described above. Chains were eluted, after resin washing, by applying onto the column 40 μL TBS pH 8.0 containing 50 mM D-maltose (Sigma-Aldrich) and incubating the resin at 25 °C for 10 min with 700 rpm shaking. Chains were collected by centrifuging the column in a 1.5 mL microcentrifuge tube for 10 s at 17,000 × *g*. For SDS/PAGE testing after each step, samples were eluted as previously described, mixed with 6× SDS loading buffer, and heated at 95 °C for 5 min. SDS/PAGE was performed on 10% (wt/vol) and 4% (wt/vol) Tris–acetate gels at 150 V.

For biotin-SpyCatcher–based assembly, 40 μL of slurry monomeric avidin resin (Thermo Scientific) was applied to a 1 mL polyprep column, rinsed with 1 mL MilliQ water, and equilibrated with 1 mL TBS pH 8.0. Biotin-SpyCatcher in TBS pH 8.0 in a final volume of 80 μL at 4 μM was added to the resin and incubated at 25 °C for 1 h with 700 rpm shaking. Unreacted biotin-SpyCatcher was removed by gravity flow, resin was washed with 1 mL wash buffer, and sequential addition of SnoopTag–AffiHER2–SpyTag and SpyCatcher–SnoopCatcher was performed as described above. After resin washing, chains were eluted by applying 40 μL of 1 mM D-biotin in TBS pH 8.0 and incubating the solution at 25 °C for 4 h with 700 rpm shaking. Chains were collected as previously indicated and analyzed by SDS/PAGE on 16% (wt/vol) and 8% (wt/vol) Tris–glycine gels with Coomassie staining.

ACKNOWLEDGMENTS. We thank Chris Schoene (University of Oxford) for biotin-SpyCatcher, University of Oxford Department of Biochemistry Biophysical Facility for assistance, and Ario de Marco (University of Nova Gorica) for Erv1p and DsbC plasmids. Funding was provided by the Medical Research Council (G.V. and J.Y.), Merton College Oxford (G.V.), Sony (T.N.), the Ecole Normale Supérieure de Lyon (R.V.G.), the Royal Society (C.V.R.), and European Research Council Grant ERC-2013-CoG 615945-PeptidePadlock (to M.D.B. and M.H.).

1. Kiessling LL, Gestwicki JE, Strong LE (2006) Synthetic multivalent ligands as probes of signal transduction. *Angew Chem Int Ed Engl* 45(15):2348–2368.
2. Bachmann MF, Jennings GT (2010) Vaccine delivery: A matter of size, geometry, kinetics and molecular patterns. *Nat Rev Immunol* 10(11):787–796.
3. Gradišar H, et al. (2013) Design of a single-chain polypeptide tetrahedron assembled from coiled-coil segments. *Nat Chem Biol* 9(6):362–366.
4. Fletcher JM, et al. (2013) Self-assembling cages from coiled-coil peptide modules. *Science* 340(6132):595–599.
5. Zaher HS, Green R (2009) Fidelity at the molecular level: Lessons from protein synthesis. *Cell* 136(4):746–762.
6. Baneyx F, Mujacic M (2004) Recombinant protein folding and misfolding in Escherichia coli. *Nat Biotechnol* 22(11):1399–1408.
7. Fairhead M, et al. (2014) SpyAvidin hubs enable precise and ultrastable orthogonal nanoassembly. *J Am Chem Soc* 136(35):12355–12363.
8. Pengo P, et al. (2010) Solid-phase preparation of protein complexes. *J Mol Recognit* 23(6):551–558.
9. Arfi Y, Shamshoum M, Rogachev I, Peleg Y, Bayer EA (2014) Integration of bacterial lytic polysaccharide monooxygenases into designer cellulosomes promotes enhanced cellulose degradation. *Proc Natl Acad Sci USA* 111(25):9109–9114.
10. Russell J, Colpitts T, Holets-McCormack S, Spring T, Stroupe S (2004) Defined protein conjugates as signaling agents in immunoassays. *Clin Chem* 50(10):1921–1929.
11. Rossi EA, Goldenberg DM, Chang CH (2012) Complex and defined biostructures with the dock-and-lock method. *Trends Pharmacol Sci* 33(9):474–481.
12. Patterson DM, Nazarova LA, Prescher JA (2014) Finding the right (bioorthogonal) chemistry. *ACS Chem Biol* 9(3):592–605.
13. Merrifield RB (1963) Solid phase peptide synthesis. 1. The synthesis of a tetrapeptide. *J Am Chem Soc* 85(14):2149–2154.
14. Marshall GR (2003) Solid-phase synthesis: A paradigm shift. *J Pept Sci* 9(9):534–544.
15. Cheloha RW, Maeda A, Dean T, Gardella TJ, Gellman SH (2014) Backbone modification of a polypeptide drug alters duration of action in vivo. *Nat Biotechnol* 32(7):653–655.
16. Letsinger RL, Mahadevan V (1965) Oligonucleotide synthesis on a polymer support. *J Am Chem Soc* 87:3526–3527.
17. Kosuri S, Church GM (2014) Large-scale de novo DNA synthesis: Technologies and applications. *Nat Methods* 11(5):499–507.
18. Raibaut L, et al. (2013) Highly efficient solid phase synthesis of large polypeptides by iterative ligations of bis(2-sulfanylethyl)amido (SEA) peptide segments. *Chem Sci (Camb)* 4(10):4061–4066.
19. Jbara M, Seenaiah M, Brik A (2014) Solid phase chemical ligation employing a rink amide linker for the synthesis of histone H2B protein. *Chem Commun (Camb)* 50(83):12534–12537.
20. Delebecque CJ, Lindner AB, Silver PA, Aldaye FA (2011) Organization of intracellular reactions with rationally designed RNA assemblies. *Science* 333(6041):470–474.
21. Chen R, et al. (2014) Biomolecular scaffolds for enhanced signaling and catalytic efficiency. *Curr Opin Biotechnol* 28:59–68.
22. Modica JA, Skarpathiotis S, Mrksich M (2012) Modular assembly of protein building blocks to create precisely defined megamolecules. *ChemBioChem* 13(16):2331–2334.
23. Huh WK, et al. (2003) Global analysis of protein localization in budding yeast. *Nature* 425(6959):686–691.
24. Zakeri B, Howarth M (2010) Spontaneous intermolecular amide bond formation between side chains for irreversible peptide targeting. *J Am Chem Soc* 132(13):4526–4527.
25. Veggiani G, Zakeri B, Howarth M (2014) Superglue from bacteria: Unbreakable bridges for protein nanotechnology. *Trends Biotechnol* 32(10):506–512.
26. Zakeri B, et al. (2012) Peptide tag forming a rapid covalent bond to a protein, through engineering a bacterial adhesin. *Proc Natl Acad Sci USA* 109(12):E690–E697.
27. Bedbrook CN, et al. (2015) Genetically encoded spy peptide fusion system to detect plasma membrane-localized proteins in vivo. *Chem Biol* 22(8):1108–1121.
28. Izoré T, et al. (2010) Structural basis of host cell recognition by the pilus adhesin from Streptococcus pneumoniae. *Structure* 18(1):106–115.
29. Yancey PH (2004) Compatible and counteracting solutes: Protecting cells from the Dead Sea to the deep sea. *Sci Prog* 87(Pt 1):1–24.
30. Radzicka A, Wolfenden R (1996) Rates of uncatalyzed peptide bond hydrolysis in neutral solution and the transition state affinities of proteases. *J Am Chem Soc* 118(26):6105–6109.
31. Telmer PG, Shilton BH (2003) Insights into the conformational equilibria of maltose-binding protein by analysis of high affinity mutants. *J Biol Chem* 278(36):34555–34567.
32. Walker IH, Hsieh PC, Riggs PD (2010) Mutations in maltose-binding protein that alter affinity and solubility properties. *Appl Microbiol Biotechnol* 88(1):187–197.
33. Wikman M, et al. (2004) Selection and characterization of HER2/neu-binding affibody ligands. *Protein Eng Des Sel* 17(5):455–462.
34. Zhang WB, Sun F, Tirrell DA, Arnold FH (2013) Controlling macromolecular topology with genetically encoded SpyTag-SpyCatcher chemistry. *J Am Chem Soc* 135(37):13988–13997.
35. Holland PM (2014) Death receptor agonist therapies for cancer, which is the right TRAIL? *Cytokine Growth Factor Rev* 25(2):185–193.
36. Huet HA, et al. (2014) Multivalent nanobodies targeting death receptor 5 elicit superior tumor cell killing through efficient caspase induction. *MAbs* 6(6):1560–1570.
37. Kang HJ, Baker EN (2011) Intramolecular isopeptide bonds: Protein crosslinks built for stress? *Trends Biochem Sci* 36(4):229–237.
38. Shi X, et al. (2012) Quantitative fluorescence labeling of aldehyde-tagged proteins for single-molecule imaging. *Nat Methods* 9(5):499–503.
39. Shah NH, Muir TW (2014) Inteins: Nature's gift to protein chemists. *Chem Sci (Camb)* 5(1):446–461.
40. Rashidian M, Dozier JK, Distefano MD (2013) Enzymatic labeling of proteins: Techniques and approaches. *Bioconjug Chem* 24(8):1277–1294.
41. Popp MWL, Ploegh HL (2011) Making and breaking peptide bonds: Protein engineering using sortase. *Angew Chem Int Ed Engl* 50(22):5024–5032.
42. Carvajal-Vallejos P, Pallissé R, Mootz HD, Schmidt SR (2012) Unprecedented rates and efficiencies revealed for new natural split inteins from metagenomic sources. *J Biol Chem* 287(34):28686–28696.
43. Chang TK, Jackson DY, Burnier JP, Wells JA (1994) Subtiligase: A tool for semisynthesis of proteins. *Proc Natl Acad Sci USA* 91(26):12544–12548.
44. Sasmal PK, et al. (2012) Catalytic azide reduction in biological environments. *ChemBioChem* 13(8):1116–1120.
45. van den Bosch SM, et al. (2013) Evaluation of strained alkynes for Cu-free click reaction in live mice. *Nucl Med Biol* 40(3):415–423.
46. Versteegen RM, Rossin R, ten Hoeve W, Janssen HM, Robillard MS (2013) Click to release: Instantaneous doxorubicin elimination upon tetrazine ligation. *Angew Chem Int Ed Engl* 52(52):14112–14116.
47. Aerni HR, Shifman MA, Rogulina S, O'Donoghue P, Rinehart J (2015) Revealing the amino acid composition of proteins within an expanded genetic code. *Nucleic Acids Res* 43(2):e8.
48. Schneider T, et al. (2014) Dissecting ubiquitin signaling with linkage-defined and protease resistant ubiquitin chains. *Angew Chem Int Ed Engl* 53(47):12925–12929.
49. Trang VH, et al. (2012) Nonenzymatic polymerization of ubiquitin: Single-step synthesis and isolation of discrete ubiquitin oligomers. *Angew Chem Int Ed Engl* 51(52):13085–13088.
50. Moyal T, Bavikar SN, Karthikeyan SV, Hemantha HP, Brik A (2012) Polymerization behavior of a bifunctional ubiquitin monomer as a function of the nucleophile site and folding conditions. *J Am Chem Soc* 134(38):16085–16092.
51. Krueger AT, Kroll C, Sanchez E, Griffith LG, Imperiali B (2014) Tailoring chimeric ligands for studying and biasing ErbB receptor family interactions. *Angew Chem Int Ed Engl* 53(10):2662–2666.
52. Dushek O, Goyette J, van der Merwe PA (2012) Non-catalytic tyrosine-phosphorylated receptors. *Immunol Rev* 250(1):258–276.
53. Shaw A, et al. (2014) Spatial control of membrane receptor function using ligand nanocalipers. *Nat Methods* 11(8):841–846.
54. Chen AY, et al. (2014) Synthesis and patterning of tunable multiscale materials with engineered cells. *Nat Mater* 13(5):515–523.
55. Sun F, Zhang WB, Mahdavi A, Arnold FH, Tirrell DA (2014) Synthesis of bioactive protein hydrogels by genetically encoded SpyTag-SpyCatcher chemistry. *Proc Natl Acad Sci USA* 111(31):11269–11274.
56. Botyanszki Z, Tay PK, Nguyen PQ, Nussbaumer MG, Joshi NS (2015) Engineered catalytic biofilms: Site-specific enzyme immobilization onto E. coli curli nanofibers. *Biotechnol Bioeng* 112(10):2016–2024.
57. Fierer JO, Veggiani G, Howarth M (2014) SpyLigase peptide-peptide ligation polymerizes affibodies to enhance magnetic cancer cell capture. *Proc Natl Acad Sci USA* 111(13):E1176–E1181.
58. Kuhlman B, Yang HY, Boice JA, Fairman R, Raleigh DP (1997) An exceptionally stable helix from the ribosomal protein L9: Implications for protein folding and stability. *J Mol Biol* 270(5):640–647.
59. Li L, Fierer JO, Rapoport TA, Howarth M (2014) Structural analysis and optimization of the covalent association between SpyCatcher and a peptide Tag. *J Mol Biol* 426(2):309–317.
60. Eigenbrot C, Ultsch M, Dubnovitsky A, Abrahmsén L, Härd T (2010) Structural basis for high-affinity HER2 receptor binding by an engineered protein. *Proc Natl Acad Sci USA* 107(34):15039–15044.
61. Friedman M, et al. (2007) Phage display selection of Affibody molecules with specific binding to the extracellular domain of the epidermal growth factor receptor. *Protein Eng Des Sel* 20(4):189–199.
62. Li J, et al. (2010) Selection of affibody molecules to the ligand-binding site of the insulin-like growth factor-1 receptor. *Biotechnol Appl Biochem* 55(2):99–109.
63. Lendel C, Dogan J, Härd T (2006) Structural basis for molecular recognition in an affibody:affibody complex. *J Mol Biol* 359(5):1293–1304.
64. Veggiani G, de Marco A (2011) Improved quantitative and qualitative production of single-domain intrabodies mediated by the co-expression of Erv1p sulfhydryl oxidase. *Protein Expr Purif* 79(1):111–114.
65. Fairhead M, Howarth M (2015) Site-specific biotinylation of purified proteins using BirA. *Methods Mol Biol* 1266:171–184.
66. Castaño-Cerezo S, Bernal V, Röhrig T, Termeer S, Cánovas M (2015) Regulation of acetate metabolism in Escherichia coli BL21 by protein N(ε)-lysine acetylation. *Appl Microbiol Biotechnol* 99(8):3533–3545.
67. Geoghegan KF, et al. (1999) Spontaneous alpha-N-6-phosphogluconoylation of a "His tag" in Escherichia coli: The cause of extra mass of 258 or 178 Da in fusion proteins. *Anal Biochem* 267(1):169–184.
68. Pringle SD, et al. (2007) An investigation of the mobility separation of some peptide and protein ions using a new hybrid quadrupole/travelling wave IMS/oa-ToF instrument. *Int J Mass Spectrom* 261(1):1–12.
69. Hernández H, Robinson CV (2007) Determining the stoichiometry and interactions of macromolecular assemblies from mass spectrometry. *Nat Protoc* 2(3):715–726.

Supporting Information

Veggiani et al. 10.1073/pnas.1519214113

SI Materials and Methods

Cloning. KOD Hot Start DNA Polymerase (Roche) was used to perform all PCRs and site-directed mutagenesis. Gibson Assembly Master Mix (New England BioLabs) was used according to the manufacturer's instructions. Constructs were initially cloned into chemically competent *E. coli* DH5α (Life Technologies).

pET28a SpyTag-MBP (Addgene plasmid ID 35050), GST-BirA, and pDEST14-SpyCatcher (GenBank JQ478411, Addgene plasmid ID 35044) have been described (26).

pET28a SnoopCatcher (GenBank accession no. KU500646, Addgene plasmid ID 72322) was generated by DNAWorks primer-mediated assembly from residues 749–860 of *S. pneumoniae* adhesin RrgA (numbering based on PDB ID code 2WW8) (28), digested with HindIII and NdeI and subcloned into pET28a. To optimize reaction with SnoopTag, the G842T mutation was made in this construct by QuikChange with 5′-GTGCCGCAGGATATTCCGGCTACATATGAATTTACCAACG and the D848G mutation with 5′-GCTACATATGAATTTACCAACGGTAAACATTATATCACCAATGAACC and their reverse complements. SnoopCatcher is 132 residues long (assuming fMet cleavage) and has an N-terminal thrombin cleavage site and His_6 tag. pET28a SnoopCatcher NA was produced from pET28a SnoopCatcher by QuikChange of N854 to A using the forward primer 5′-ACATTATATCACCGCTGAACCGATACCGCCG and its reverse complement.

pET28a SnoopTag-MBP (GenBank accession no. KU356870, Addgene plasmid ID 72323) was generated in two steps. We first cloned the reactive peptide based on the N-terminal β-strand of RrgA's D4 domain (residues 734–748) (28) into pET28a SpyTag-MBP (26) by site-directed, ligase-independent mutagenesis (SLIM) PCR using 5′-GGTAGTGGTGAAAGTGGTAAAATCGAAGAAG, 5′-AAACTGGGCGATATTGAATTTATTAAAGTGAACAAAAACGATAAAGGTAGTGGTGAAAGTGGTAAAATCGAAGAAG, 5′-TCCCATATGGCTGCCGCGCG, and 5′-TTTATCGTTTTTGTTCACTTTAATAAATTCAATATCGCCCAGTTTTCCCATATGGCTGCCGCGCG. We then removed the three C-terminal residues of the peptide to generate SnoopTag (residues 734–745) using QuikChange with 5′-GAATTTATTAAAGTGAACAAAGGTAGTGGTGAAAGTGGTAAAATCG and its reverse complement. pET28a SnoopTag KA-MBP, an unreactive version of SnoopTag, was generated by QuikChange of K742 to A on pET28a SnoopTag-MBP using 5′-GGGCGATATTGAATTTATTGCAGTGAACAAAGGTAGTGG and its reverse complement.

pET28a MBP-SpyCatcher was generated by fusing SpyCatcher with a Gly/Ser spacer at the C terminus of MBP through overlap extension PCR. SpyCatcher was amplified from pDEST14-SpyCatcher (26) using the forward primer 5′-GTTCGGGCGGTAGTGGTGCCATGGTTGATACCTTATCAGGTTTATCAAGTGAGCAAG and the reverse primer 5′-TACTAAGCTTCTATTAAATATGAGCGTCACCTTTAGTTGCTTTGCCATTTACAG. The forward primer 5′-ATCTCATATGGGCAGCAGCCATCATCATCATCATCAC and the reverse primer 5′-GTATCAACCATGGCACCACTACCGCCCGAACCCGAGCTCGAATTAGTCTGCG were used to amplify MBP from pET28a SpyTag-MBP (26). The two resulting PCR products were mixed and amplified again using the SpyCatcher forward primer and the MBP reverse primer, digested with NdeI and HindIII, and subcloned into pET21. To increase the affinity of MBP-SpyCatcher for amylose, we first made the A312V and I317V mutations in MBP, previously shown to improve maltose binding (32), by QuikChange using the forward primer 5′-GTCTTACGAGGAAGAGTTGGTGAAAGATCCACGTGTGGCCGCCACTATGGAAAACGC and its reverse complement. We then deleted residues 172, 173, 175, and 176 from MBP, previously shown to improve maltose binding (31), using QuikChange with 5′-GGGTTATGCGTTCAAGTATGGCGACATTAAAGACGTGGGCG and its reverse complement. To decrease even further the dissociation from amylose resin, we generated tandem fusions of A312V I317V del 172, 173, 175, 176 MBP (MBPmt) to give pET21 MBPx-SpyCatcher (N-terminal His_6 tag–MBPmt–spacer–MBPmt–spacer–SpyCatcher) (GenBank accession no. KU361183, Addgene plasmid ID 72327) via Gibson assembly.

pET28a SpyCatcher–SnoopCatcher (GenBank accession no. KU361182, Addgene plasmid ID 72324) was produced in steps. Initially SpyCatcher was fused with a Gly/Ser spacer at the N terminus of SnoopCatcher. Then, the Gly/Ser spacer was replaced with an α-helical spacer (sequence PANLKALEAQKQKEQRQAAEELANAKKLKEQLEK) (58). The forward primer 5′-CTTTAAGAAGGAGATATACATATGTCGTACTACCATCACCATC and the reverse primer 5′-CCGCTGCTTCCGGATCCAATATGAGCGTCACCTTTAGTTG were used to amplify the SpyCatcher portion from pDEST14 SpyCatcher. The SnoopCatcher part was cloned using the forward primer 5′-CATATTGGATCCGGAAGCAGCGGCCTGGTGCCGCGCGGATCCCATATGAAGCCGCTGC and the reverse primer 5′-GTGGTGGTGGTG-GTGCTCGAGTTATTATTTCGGCGGTATCGGTTC from pET28a SnoopCatcher. Following SpyCatcher and SnoopCatcher fusion, the Gly/Ser spacer was replaced with a stable monomeric α-helical linker using the forward primer 5′-CTAAAGGTGACGCTCATATTGGATCCCCCGCCAACCTGAAGGCCCTGGAGGCCCAGAAGCAGAAGGAGCAGAGACAGGCCGCCGAGGAGC and the reverse primer 5′-CACGGCACCACGCAGCGGCTTCATATGGGATCCCTTCTCCAGCTGCTCCTTCAGCTTCTTGGCGTTGGCCAGCTCCTCGGCGGCCTGTC. Thirty-five residues were deleted from SpyCatcher's N terminus (59) via QuikChange using the forward primer 5′-CACCATCACCATCACGATTACGATAGTGCTACCCATATTAAATTCTC and its reverse complement.

pET28a SnoopTag–AffiHER2–SpyTag (N-terminal His_6–SnoopTag–spacer–Affibody against HER2–spacer–SpyTag) (GenBank accession no. KU296975) was generated by Gibson assembly using the forward primer 5′-GTGAACAAAGGCAGTGGTGAGTCGGGATCCGGAGCTAGCATGACTGGTGG and the reverse primer 5′-CATCACGATGTGGGCACCGGAACCTTCCCCGGATCCCTCGAGGCCTTTCGG from pET28a KTag–AffiHER2–SpyTag (57, 60).

pET28a SnoopTag–AffiEGFR–SpyTag (GenBank accession no. KU296973), containing an affibody against human EGFR (61), was generated by inverse PCR from pET28a SnoopTag–AffiHER2–SpyTag using 5′-CCTAATCTGAATGGATGGCAGATGACCGCTTTTATTGCCTCTCTTGTTGATGACCCAAGCCAAAGCGC and 5′-GAGGTTTGTATTTCCTCCCATGCAGCCCACATTTCTTTGTTGAATTTGTTGTCCACGCC.

pET28a SnoopTag–AffiIGF1R–SpyTag (GenBank accession no. KU296974), containing an affibody against human IGF1R (62), was generated by inverse PCR with the primers 5′-TAAATCGAAAACAGTCTACCGCATTTATTTCTAGCCTTGAAGATGACCCAAGCCAAAGCGCTAACC and 5′-GATTCGGTAATGCCAGGATTTCGATTGCAGCATAGAAACCTTCTTTGTTGAATTTGTTGTCCACGCCCG from pET28a SnoopTag–AffiHER2–SpyTag.

pET28a SnoopTag–AffiTaq–SpyTag, containing an affibody against Taq DNA polymerase (63), was generated from pET28a SnoopTag–AffiHER2–SpyTag by inverse PCR using the primers 5′-CTACCCAACCTAAACGGGGTACAAGTAAAGGCTTTCATAGACTCGCTAAGGGATGACCCAAGCCAAAGCGC and 5′-GTTGAATATCTCCCAAGTAGCCCACCCTAGCTCCTTGTTGAACTTGTTGTCTACTTCTTTGTTGAATTTGTTGTCCACGCC.

pET28a SnoopTag–SpyTag–AffiHER2 × 3 (GenBank accession no. KU296976) (N-terminal His_6 tag–SnoopTag–spacer–SpyTag–three tandem repeats of Affibody against HER2 connected by Gly/Ser spacers) was synthesized as a gBlocks gene fragment (Integrated DNA Technologies) and inserted into pET28 by Gibson assembly using the forward primer 5′-TGAGATCCGGCTGCTAACAAAGC and the reverse primer 5′-CACCAGGCCGCTGCTGTG.

pET28a SnoopTag–anti-DR5–SpyTag (GenBank accession no. KU500643) based on the 4E6 nanobody against human DR5 with a C-terminal His_6 tag and designed for expression in the cytosol of *E. coli* was synthesized via GeneArt Gene Synthesis (Life Technologies); a nanobody is a single domain from the variable region of a heavy chain-only camelid-derived antibody (36).

pET28a SnoopTag–monomeric enhanced green fluorescent protein (mEGFP)–SpyTag (GenBank accession no. KU500644, Addgene plasmid ID 72325) was cloned by substituting mEGFP at the *BamHI* sites in pET28a SnoopTag–AffiHER2–SpyTag and by PCR to extend the spacer.

AviTag–SpyCatcher (GenBank accession no. KU500645, Addgene plasmid ID 72326), containing a peptide tag for site-specific biotinylation at the N terminus, was cloned by SLIM PCR from pDEST14 SpyCatcher (26) using 5′-GATTACGACATCCCAACGACCGAAAACCTG, 5′-GCCTGAACGATATTTTTGAAGCGCAGAAAA-TTGAATGGCATGAAGGCGATTACGACATCCCAACGACCGAAAACCTG, 5′-GTGATGGTGATGGTGATGGTAGTACGACATATG, and 5′-TGCCATTCAATTTTCTGCGCTTCAAAAATATCGTTCAGGCCGCTGCCGTGATGGTGATGGTGATGGTAGTACGACATATG.

All mutations and constructs were verified by sequencing.

Protein Expression and Purification. Proteins were expressed in *E. coli* BL21 DE3 RIPL (Agilent) with the exception of SnoopTag–anti-DR5–SpyTag, which was expressed in *E. coli* BL21 DE3 transformed with a plasmid for the expression of the Erv1p sulfhydryl oxidase and the disulfide bond isomerase DsbC (a kind gift of Ario de Marco, University of Nova Gorica, Nova Gorica, Slovenia), facilitating accurate disulfide bond formation (64). Colonies were grown overnight at 37 °C in Luria–Bertani broth (LB) containing 0.5 mg/mL kanamycin for pET28a vectors and 0.1 mg/mL ampicillin for pET21 vectors. For SnoopTag–anti-DR5–SpyTag expression, colonies were inoculated overnight at 37 °C in LB containing 0.5 mg/mL kanamycin and 3.4 μg/mL chloramphenicol. The overnight cultures were diluted 1:100 in LB containing 0.8% (wt/vol) glucose with the appropriate antibiotic, grown at 37 °C at 200 rpm (all bacterial shaking with 2.5-cm throw) to OD_{600} 0.5–0.6, and induced with 0.4 mM IPTG at 30 °C at 200 rpm for 4 h.

To express SnoopTag– anti-DR5–SpyTag, cultures were grown at 37 °C at 200 rpm to OD_{600} 0.4. Erv1p and DsbC expression was induced with 0.5% (wt/vol) arabinose, and the temperature was lowered to 30 °C at 200 rpm for 45 min. After 45 min, 0.4 mM IPTG was added to induce nanobody expression, and bacteria were grown at 30 °C at 200 rpm for 4 h.

Proteins were purified by standard methods on Ni-NTA (Qiagen) and dialyzed thrice with TBS (50 mM Tris·HCl and 50 mM NaCl) pH 8.0.

For MBPx-SpyCatcher's purification, after elution from Ni-NTA, the buffer was exchanged by dialysis into 20 mM Tris·HCl pH 8.0 at 4 °C, loaded onto quaternary high-performance resin (GE Healthcare), and eluted by 10 column volumes (i.e., 10 mL) of linear gradient of 0–0.15 M NaCl with a flow rate of 1 mL/min. An extra elution step was performed with a linear gradient of 0.15–0.35 M NaCl at the flow rate of 1.5 mL/min and collecting 0.5 mL fractions. Collected fractions were dialyzed into TBS, concentrated using a Vivaspin centrifugal concentrator 5 kDa cutoff (GE Healthcare), and stored at −80 °C.

Ni-NTA purified affibodies were dialyzed in 20 mM 2-(*N*-morpholino)ethanesulfonic acid pH 5.8 at 4 °C and loaded onto sulfopropyl high performance resin (GE Healthcare). Protein was eluted by applying a linear gradient of 0.2–0.5 M NaCl and collecting 1 mL fractions. The eluted fractions were concentrated to 1–2 mg/mL using a Vivaspin centrifugal concentrator 5 kDa cutoff (GE Healthcare), dialyzed into TBS pH 8.0, and stored at −80 °C.

For SpyCatcher–SnoopCatcher's purification, after elution from Ni-NTA, the buffer was exchanged by dialysis into 20 mM Tris·HCl pH 8.0 at 4 °C, loaded onto quaternary high performance resin, and eluted with a linear gradient of 0.2–0.5 M NaCl. Collected fractions were dialyzed into TBS, concentrated using a Vivaspin centrifugal concentrator 5 kDa cutoff (GE Healthcare), and stored at −80 °C.

Biotin–SpyCatcher was generated by biotinylating purified AviTag–SpyCatcher in PBS (10 mM Na_2HPO_4, 137 mM NaCl, 27 mM KCl, 1.8 mM KH_2PO_4 pH 7.4) containing 5 mM $MgCl_2$, 1 mM ATP, 380 μM D-biotin, and 7 μM GST-BirA for 1 h at 25 °C. After 1 h of incubation, further GST-BirA was added to give a final concentration of 14 μM, and the reaction was incubated for an extra 1 h at 25 °C. GST-BirA was removed by incubating with 50 μL of slurry Hi-Cap Glutathione matrix (Qiagen) at 25 °C, with end-over-end rotation for 30 min. Resin was spun down at 4,000 × *g* for 1 min and supernatant collected and dialyzed overnight at 4 °C into PBS. To confirm complete biotinylation, a streptavidin gel-shift assay was performed as described (65).

Isopeptide Bond Reconstitution Conditions. SnoopTag reaction to completion was tested by mixing SnoopTag-MBP and SnoopCatcher in TBS pH 8.0 containing 1.5 M TMAO and incubating the solution at 25 °C for various times. A 1:1 reaction contained 10 μM SnoopTag-MBP and 10 μM SnoopCatcher. A 2:1 reaction contained 10 μM SnoopTag-MBP and 20 μM SnoopCatcher. Reactions were stopped in SDS loading buffer, as described above, before SDS/PAGE. The % SnoopTag reacted was calculated as 100 × [1 − (SnoopTag band intensity in the presence of SnoopCatcher)/(SnoopTag band intensity in the absence of SnoopCatcher)].

SnoopCatcher reaction to completion was tested by mixing SnoopTag-MBP and SnoopCatcher in TBS pH 8.0 containing 1.5 M TMAO and incubating the solution at 25 °C for various times. A 1:1 reaction contained 10 μM SnoopTag-MBP and 10 μM SnoopCatcher. A 2:1 reaction contained 20 μM SnoopTag-MBP and 10 μM SnoopCatcher. A 4:1 reaction contained 40 μM SnoopTag-MBP and 10 μM SnoopCatcher. Reactions were stopped in SDS loading buffer, as described above, before SDS/PAGE. The % SnoopCatcher reacted was calculated as 100 × [1 − (SnoopCatcher band intensity in the presence of SnoopTag)/(SnoopCatcher band intensity in the absence of SnoopTag)].

The % Reconstitution was calculated as 100× the band intensity of the covalent adduct, divided by the sum of band intensities of SnoopTag-MBP, SnoopCatcher, and the SnoopTag-MBP:SnoopCatcher covalent adduct.

To evaluate the pH dependence of reaction between SnoopTag-MBP and SnoopCatcher, each protein was mixed at 10 μM in succinate–phosphate–glycine buffer (12.5 mM succinic acid, 43.75 mM NaH_2PO_4, 43.75 mM glycine; pH was adjusted using NaOH), chosen to enable suitable buffering over a broad pH

range, ranging from pH 4.0 to pH 9.0, and incubated at 25 °C for 15 min.

To determine the effect of temperature, 10 μM SnoopTag-MBP and 10 μM SnoopCatcher were mixed for 15 min at the indicated temperatures in PBS pH 8.0 containing 1.5 M TMAO. PBS was used in place of TBS because the pH of Tris buffers changes substantially with temperature.

To test orthogonality, 10 μM SnoopTag-MBP and 10 μM SnoopCatcher or SpyCatcher were incubated for 18 h at 25 °C in TBS pH 8.0, before SDS/PAGE. Similarly 10 μM SpyTag-MBP and 10 μM SnoopCatcher or SpyCatcher were incubated as above.

To investigate the sensitivity to the buffer composition, SnoopTag-MBP and SnoopCatcher each at 10 μM were incubated at 25 °C for 15 min in PBS pH 8.0, TBS pH 8.0, or TBS pH 8.0 containing 1% Triton X-100 (wt/vol), 1% Tween-20 (vol/vol), 10 mM ethylene diamine tetraacetate (EDTA), 10 mM $MgCl_2$, 10 mM DTT, or 50 mM Tris·HCl pH 8.0 with 1 M NaCl.

To test TMAO dependence, SnoopTag-MBP and SnoopCatcher each at 10 μM were incubated at 25 °C for 15 min in TBS pH 8.0 with the indicated concentration of TMAO, before SDS/PAGE.

To test reversibility, 10 μM SnoopCatcher or SnoopCatcher NA was incubated with 15 μM SnoopTag-MBP for 6 h, and then SnoopTag–AffiHER2–SpyTag at a final concentration of 130 μM was added for 16 h, all at 25 °C in PBS pH 8.0. To test the effect of competing ammonia, 10 μM SnoopTag-MBP and 10 μM SnoopCatcher were incubated for 2 h at 25 °C in TBS pH 8.0 with 1.5 M TMAO before ammonium chloride pH 9.0 was added to a final concentration of 1 M for a further 16 h at 25 °C.

To test SpyCatcher/SpyTag completion, 20 μM SnoopTag–mEGFP–SpyTag was incubated with 40 μM SpyCatcher for 120 min in 40 mM Na_2HPO_4 and 20 mM citric acid at pH 5.0 at 25 °C. To test SpyCatcher with excess SpyTag-MBP, 10 μM SpyCatcher was incubated with 20 μM SpyTag-MBP for 32 min at 25 °C in TBS pH 8.0.

Mass Spectrometry. We incubated 100 μM SnoopTag solid-phase synthesized peptide (GKLGDIEFIKVNKGY, Insight Biotechnology) and 50 μM SnoopCatcher at 25 °C for 3 h in PBS pH 7.4. Mass spectrometry analysis was performed using a Micromass LCT time-of-flight electrospray ionization mass spectrometer (Micromass), and *m/z* spectrum was converted to molecular mass profile using a maximum entropy algorithm and the V4.00.00 software (Waters). ExPASy ProtParam was used to predict the molecular masses based on the protein's amino acid sequence, with the N-terminal fMet cleaved and subtracting 17.0 Da for isopeptide bond formation by SnoopTag and 18.0 Da for isopeptide bond formation by SpyTag. Acetylation and gluconylation are commonly found side reactions for proteins overexpressed in *E. coli* BL21 (66, 67).

For MS of the AffiHER2 polyprotein, the chain was concentrated to ∼5 μM and buffer-exchanged into 250 mM ammonium acetate using an Amicon Ultra 0.5 mL centrifugal filter with a 100 kDa cutoff (Millipore). Measurements were carried out on a first-generation Synapt High Definition Mass Spectrometry Quadrupole Time of Flight mass spectrometer (Waters) (68), calibrated using 10 mg/mL caesium iodide in 250 mM ammonium acetate. We delivered 2.5 μL aliquots of sample by nano-electrospray ionization via gold-coated capillaries, prepared in house (69). Instrumental parameters were as follows: source pressure, 6.0 mbar; capillary voltage, 1.20 kV; cone voltage, 150 V; trap energy, 60 V; transfer energy, 12 V; bias voltage, 5 V; trap pressure, 0.022 mbar. Mass spectra were smoothed and peak-centered, and masses were assigned using MassLynx v4.1 (Waters).

Size-Exclusion Chromatography. AffiHER2 chains were analyzed by size-exclusion chromatography on a Superdex 200 GL 10/300 column (24 mL bed volume) (GE Healthcare). The column was calibrated using standards from 660 kDa to 1.35 kDa (thyroglobulin, IgG, ovalbumin, myoglobin, and vitamin B12) (Bio-Rad). Samples were eluted at 0.4 mL/min in 50 mM Tris·HCl with 500 mM NaCl pH 8.0, with absorbance profile measured at 280 nm on an ÄKTA Purifier 10 at 4 °C (GE Healthcare).

Cell Culture. MDA–MB-231 cells (human breast cancer cell line) were from American Type Culture Collection and were grown at 37 °C with 5% CO_2 in Dulbecco's Modified Eagle Medium (DMEM) (Life Technologies) containing 10% (vol/vol) FCS (Sigma-Aldrich) and 50 U/mL penicillin and 50 μg/mL streptomycin (Sigma-Aldrich). Cells were passaged for less than 6 mo.

Stability Testing of Chains. For temperature-stability testing, MBPx-SpyCatcher:(SnoopTag–AffiHER2–SpyTag:SpyCatcher–SnoopCatcher)$_4$:SnoopTag–AffiHER2–SpyTag chains in 150 mM ammonium acetate pH 8.0 at 3 μM in a final volume of 30 μL were incubated at 25, 37, 50, 60, or 70 °C for 3 min and then cooled to 10 °C at 3 °C/s in a Bio-Rad C1000 Thermal Cycler. Samples were then spun at 17,000 × *g* at 4 °C for 30 min to remove aggregates, and the supernatant was analyzed by SDS/PAGE on an 8% (wt/vol) Tris–glycine gel. For time-dependent stability testing, decamer chains at 3 μM in TBS pH 8.0 containing 0.1% sodium azide, 1 mM phenylmethylsulfonyl fluoride, 1 mM EDTA, and EDTA-free mixed protease inhibitors (Roche) in a final volume of 40 μL were incubated at 25 °C for 24 or 96 h. At each time point, the samples were spun at 17,000 × *g* at 4 °C for 30 min, and the supernatant was analyzed by SDS/PAGE on an 8% (wt/vol) Tris–glycine gel with Coomassie staining.

Combinatorial Assembly of Chains. We applied 40 μL per well of slurry amylose resin (New England BioLabs) to an AcroPrep Advance 1 mL 96-well plate with a 0.45 μm GHP (hydrophilic polypropylene) membrane (Pall). Resin was rinsed with 1 mL MilliQ water and equilibrated with 1 mL TBS pH 8.0. We added 160 pmol MBPx-SpyCatcher in TBS pH 8.0 in a final volume of 80 μL to the resin and incubated the resin at 25 °C for 1 h with 1,000 rpm shaking on a ThermoMixer comfort. Unreacted protein was removed from the resin by centrifugation at 218 × *g* at 25 °C for 1 min. To wash the resin, 1 mL of wash buffer was applied to each well and discarded by centrifugation at 218 × *g* at 25 °C for 1 min. We added 2.4 nmol SnoopTag–AffiIGF1R–SpyTag, SnoopTag–AffiEGFR–SpyTag, SnoopTag–AffiTaq–SpyTag, SnoopTag–SpyTag–AffiHER2 × 3, or SnoopTag–anti-DR5–SpyTag to the resin in 40 mM Na_2HPO_4 and 20 mM citric acid pH 5.0 and incubated the resin at 25 °C for 1 h with 1,000 rpm shaking. Protein excess was removed by centrifugation at 218 × *g* at 25 °C for 1 min, and resin was washed with 1 mL wash buffer. We added 2.8 nmol SpyCatcher–SnoopCatcher in TBS pH 8.0 with 1.5 M TMAO to the resin and incubated the resin at 25 °C for 2 h with 1,000 rpm shaking. Unreacted SpyCatcher–SnoopCatcher was removed by centrifugation, and resin was washed by applying 1 mL wash buffer and spinning the 96-well plate at 218 × *g* at 25 °C for 1 min. Chains were generated, as described above, by sequential addition of SpyTag/SnoopTag-containing monomers and SpyCatcher–SnoopCatcher. Chains were eluted from the resin by applying 20 μL TBS pH 8.0 containing 100 mM D-maltose and incubating the resin at 25 °C for 10 min with 1,000 rpm shaking. Eluted chains were collected by placing the 96-well plate on top of a 96-well round-bottom polystyrene plate (Corning) and centrifuging the plates at 25 °C with 218 × *g* for 1 min. Eluted chains were analyzed by SDS/PAGE on an 8% (wt/vol) Tris–glycine gel with Coomassie staining. As expected from the molecular weight, chains containing tandem affibodies had lower mobility. The mobility of the chains with four anti-DR5 and one HER2 × 3 was greatest when the HER2 × 3 was at position 5, consistent with the less branched arrangement of such a chain following boiling in SDS, compared with having HER2 × 3 at positions 1, 2, 3, or 4 (Fig. 5*A*). Protein concentration was determined using the micro-bicinchoninic

acid protein assay kit (Pierce) according to the manufacturer's instructions.

Combinatorial Screening of Polyproteams. MDA–MB-231 cells were seeded into a 96-well plate at 40,000 per well in 50 μL DMEM containing 50 U/mL penicillin and 50 μg/mL streptomycin and incubated at 37 °C with 5% CO_2 for 16 h. We then added 50 μL polyproteam at the final concentration of 200 ng/mL in DMEM containing 2% (wt/vol) 0.2 μm-filtered BSA (Sigma-Aldrich), 50 U/mL penicillin, and 50 μg/mL streptomycin (DMEM–BSA). The plate was incubated at 37 °C with 5% CO_2 for 40 h (or for the indicated time for Fig. 5*D*), and cell viability was assessed by resazurin (Alamar Blue) assay. We added 20 μL of 0.15 mg/mL resazurin sodium salt (Sigma-Aldrich) in PBS pH 7.4, and the plate was incubated at 37 °C and 5% CO_2 for 4 h. Cell viability was determined by measuring the fluorescence of reduced resazurin (λ_{ex} 544 nm, λ_{em} 590 nm) using a SpectraMax3 plate reader (Molecular Devices). The percentage of viable cells was calculated as 100 × (signal of treated cells – signal without cells)/(signal untreated cells – signal without cells). The signal without cells was taken as the resazurin fluorescence in the absence of cells, whereas the signal of untreated cells came from the fluorescence of cells that were incubated only with DMEM–BSA.

Dose–Response Curve of Polyproteam. MDA–MB-231 cells were seeded at a density of 40,000 cells per well into a 96-well microplate in DMEM with 50 U/mL penicillin and 50 μg/mL streptomycin and incubated for 16 h at 37 °C, 5% CO_2. Cells were treated with varying concentrations of NNNNE, a polyprotein chain composed of SnoopTag–anti-DR5–SpyTag at positions 1–4 and SnoopTag–AffiEGFR–SpyTag at position 5. As a negative control, HHHHH was used at 200 ng/mL. We added 50 μL of each sample in DMEM–BSA to cells, and the plate was incubated at 37 °C with 5% CO_2 for 40 h. Viability was measured with resazurin as above.

Caspase Activation Assay. We seeded 40,000 MDA–MB-231 cells per well in a 96-well plate and incubated the cells for 16 h at 37 °C with 5% CO_2 in DMEM containing 50 U/mL penicillin and 50 μg/mL streptomycin. Cells were then cultured at 37 °C with 5% CO_2 for 1 h in the presence or absence of 20 μM Z-VAD-FMK (a pan-caspase inhibitor; Sigma-Aldrich) before addition of NNNNE, KillerTRAIL (recombinant human TRAIL with a linker peptide to promote stable trimerization; Enzo Life Sciences), or HHHHH to a final concentration of 200 ng/mL. Cells were incubated at 37 °C with 5% CO_2 for a further 5 h. The activity of caspases-3/7 was detected with the Apo-One Homogeneous Caspase-3/7 kit (Promega) by adding 100 μL caspase-3/7 reagent diluted fourfold in PBS. The plate was mixed at 500 rpm on a ThermoMixer comfort for 1 min and incubated in the dark at 25 °C for 1 h. Fluorescence was measured using a SpectraMax3 plate reader with 485 nm excitation and 530 nm emission.

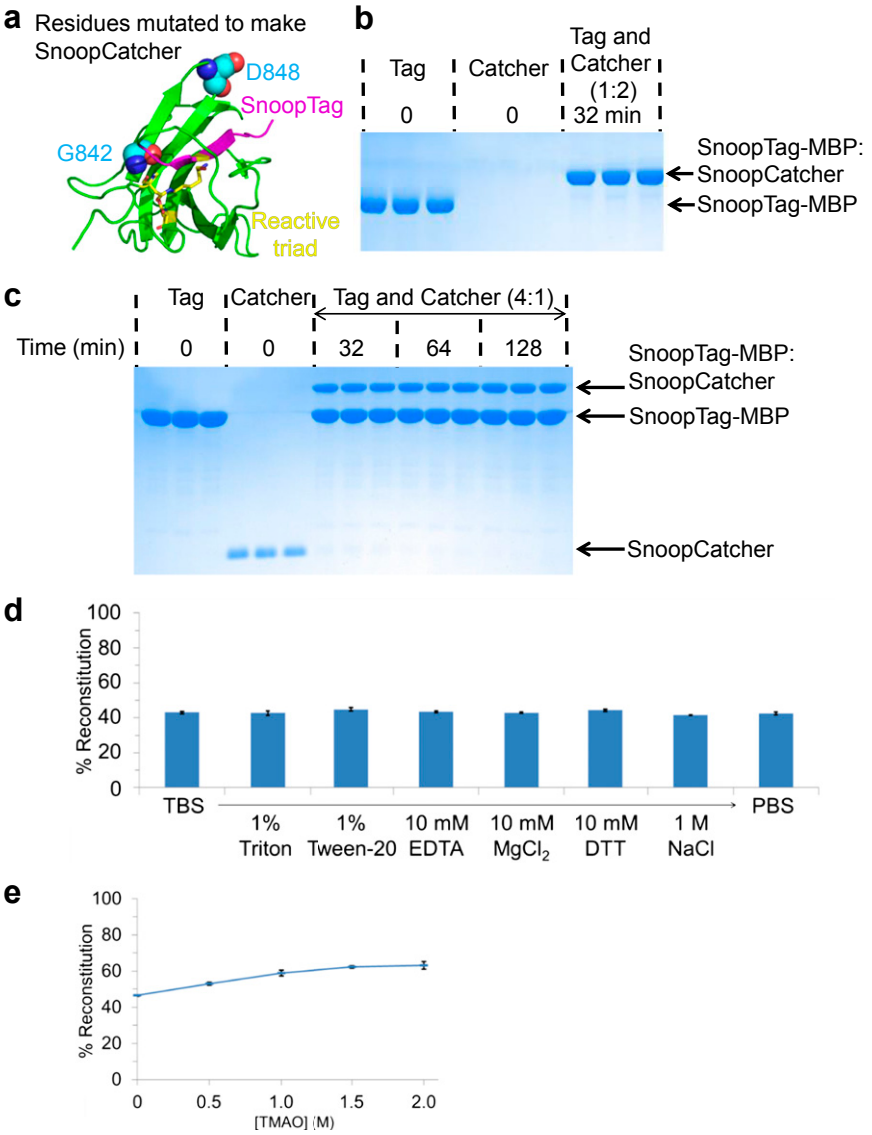

Fig. S1. SnoopTag and SnoopCatcher reaction conditions. (*A*) Point mutations to make SnoopCatcher. From the C-terminal domain of RrgA in cartoon format (based on PDB ID code 2WW8), residues mutated are shown in space-fill with carbons in cyan (G842 was changed to T and D848 to G). The Lys, Asn, and Glu involved in isopeptide bond formation are shown in stick format in yellow and the rest of SnoopTag colored magenta. (*B*) Sample gel to test for quantitative reaction of SnoopTag. Shown are 10 μM SnoopTag-MBP and 20 μM SnoopCatcher alone or mixed for 32 min (triplicate samples) before SDS/PAGE with Coomassie staining. (*C*) Sample gel to test for quantitative reaction of SnoopCatcher. Shown are 10 μM SnoopCatcher and 40 μM SnoopTag-MBP alone or mixed for the indicated times (triplicate samples) before SDS/PAGE with Coomassie staining. (*D*) Buffer dependence of SnoopTag/SnoopCatcher reaction. We incubated 10 μM SnoopTag-MBP with 10 μM SnoopCatcher at pH 8.0 for 15 min at 25 °C in the indicated buffer and analyzed the samples by SDS/PAGE with Coomassie staining. (*E*) TMAO dependence of SnoopTag/SnoopCatcher reaction tested as in *D*. Error bars are all mean ±1 SD; $n = 3$. Some error bars are too small to be visible.

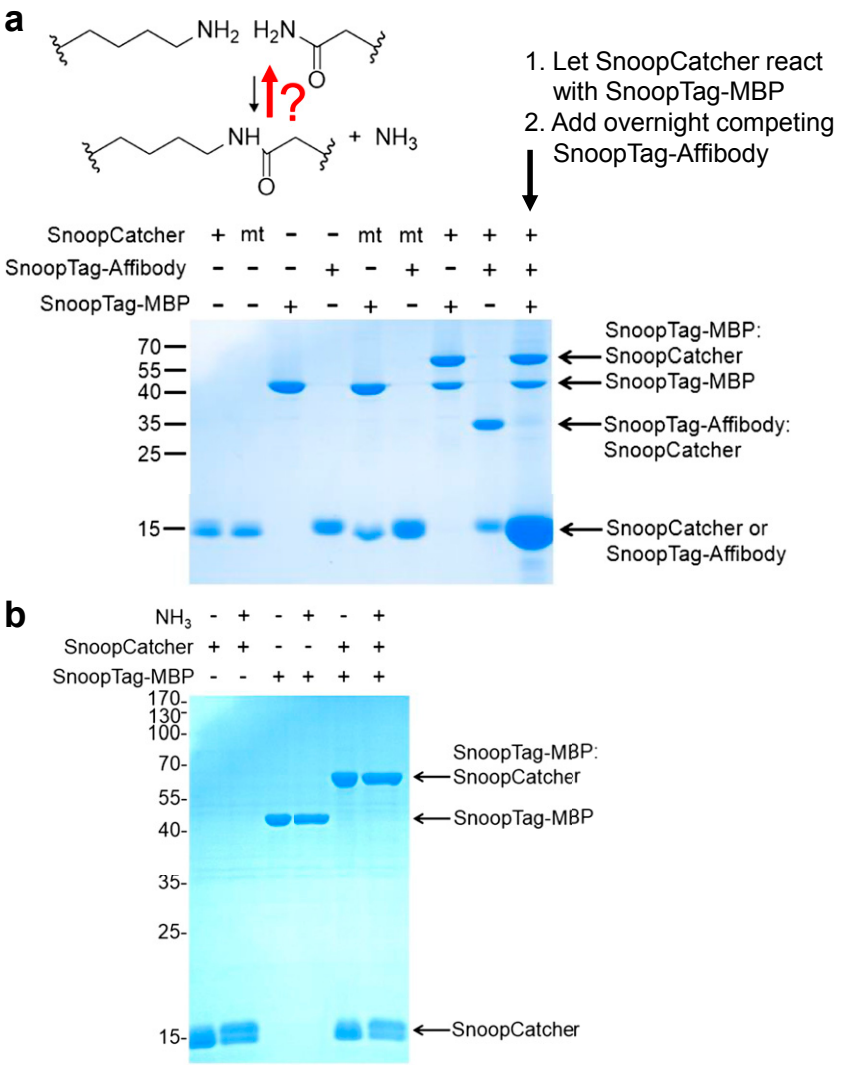

Fig. S2. SnoopCatcher reaction with SnoopTag was not reversible. (*A*) Reaction not reversed by competing SnoopTag. In lanes 1–8, SnoopCatcher, SnoopCatcher NA nonreactive control (mt), SnoopTag-MBP, and SnoopTag-Affibody (SnoopTag–AffiHER2–SpyTag) are shown alone (each at 10 μM) or after mixing for 6 h at 25 °C. In lane 9, 10 μM SnoopCatcher was reacted with 15 μM SnoopTag-MBP for 6 h, and then we added SnoopTag–AffiHER2–SpyTag to 130 μM for 16 h at 25 °C to look for SnoopTag–AffiHER2–SpyTag:SnoopCatcher formation. (*B*) Reaction not reversed by competing ammonia. We incubated SnoopTag-MBP with SnoopCatcher for 2 h in TBS with TMAO. We then added NH_4Cl pH 9.0 to a 1 M final concentration to the indicated samples ($+NH_3$) for 16 h (all at 25 °C) before SDS/PAGE with Coomassie staining. (The ammonium ion's pK_a is 9.2.)

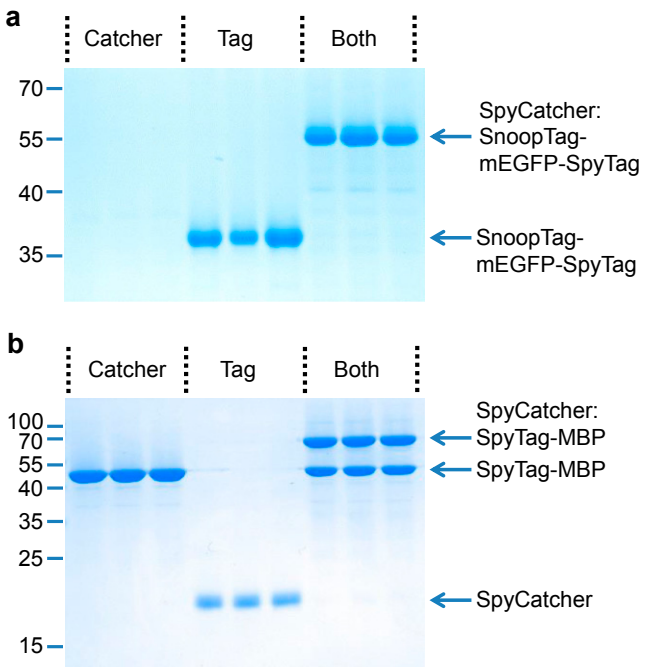

Fig. S3. SpyTag and SpyCatcher reacted to a high degree of completion. (*A*) SpyTag with excess SpyCatcher. We incubated 20 μM SnoopTag–mEGFP–SpyTag with 40 μM SpyCatcher for 120 min at 25 °C before SDS/PAGE with Coomassie staining showing triplicate samples. (*B*) SpyCatcher with excess SpyTag. We incubated 10 μM SpyCatcher with 20 μM SpyTag-MBP for 32 min at 25 °C before SDS/PAGE with Coomassie staining showing triplicate samples.

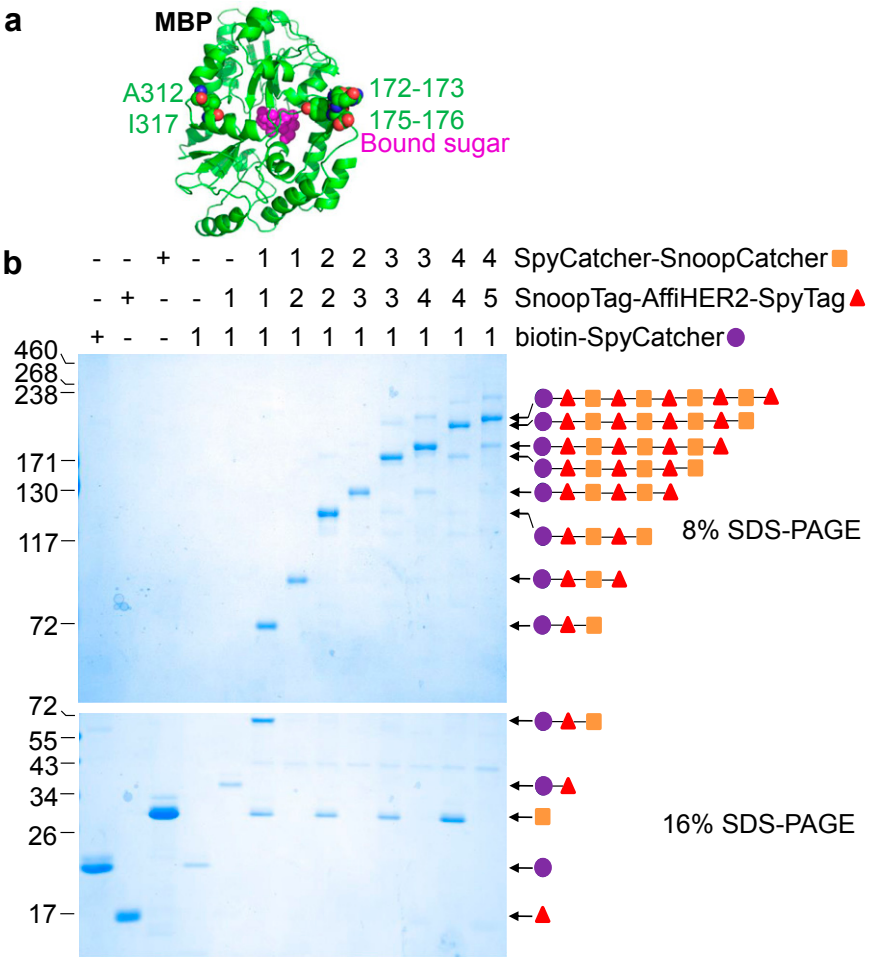

Fig. S4. Resin attachment for solid-phase polyprotein synthesis. (*A*) Location of MBP mutations, based on PDB ID code 1ANF. A312 was changed to V, I317 to V, and 172–173 and 175–176 were deleted. Mutated residues are shown in space-fill. The bound sugar part is shown in space-fill and is colored magenta. (*B*) Solid-phase polyprotein synthesis using avidin attachment. Lanes 1–3 show biotin-SpyCatcher, SnoopTag–AffiHER2–SpyTag, and SpyCatcher–SnoopCatcher in isolation. For solid-phase synthesis, biotin-SpyCatcher was bound to monomeric avidin resin. Sequential addition of SnoopTag–AffiHER2–SpyTag and SpyCatcher–SnoopCatcher led to chain formation up to a decamer. After each stage, sample was eluted from one aliquot of resin with biotin (lanes 4–13). Samples, without any further purification, were analyzed by SDS/PAGE [both 8% and 16% (wt/vol) gels] with Coomassie staining.

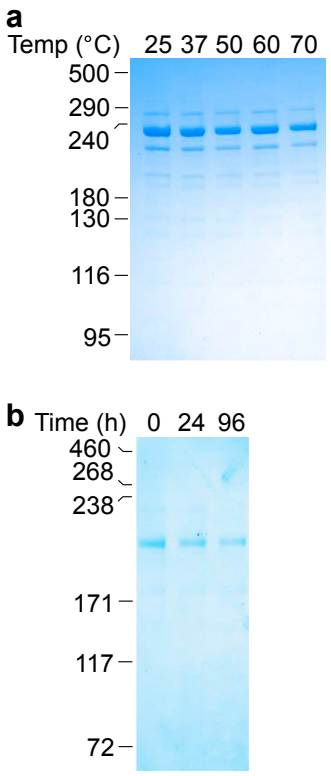

Fig. S5. Stability of polyproteins. (*A*) Decamer thermostability. MBPx-SpyCatcher:(SnoopTag–AffiHER2–SpyTag:SpyCatcher–SnoopCatcher)$_4$:SnoopTag–AffiHER2–SpyTag was incubated at the indicated temperature for 3 min, centrifuged to remove aggregates, and analyzed by SDS/PAGE with Coomassie staining. (*B*) Decamer time-dependent stability. Biotin-SpyCatcher:(SnoopTag–AffiHER2–SpyTag:SpyCatcher–SnoopCatcher)$_4$:SnoopTag–AffiHER2–SpyTag was incubated at 25 °C for the indicated time, before boiling in SDS loading buffer and analysis by SDS/PAGE with Coomassie staining.

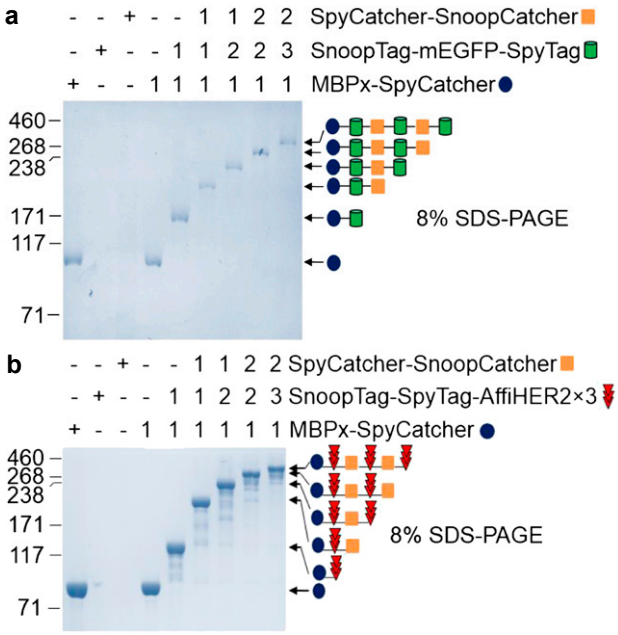

Fig. S6. Different building blocks incorporated in polyproteams. (*A*) Synthesis of fluorescent polyproteins. MBPx-SpyCatcher was bound by amylose resin and then extended iteratively with SnoopTag–mEGFP–SpyTag and SpyCatcher–SnoopCatcher. Samples were eluted at each stage with maltose and analyzed by SDS/PAGE with Coomassie staining. (*B*) Synthesis of branched polyproteins, as for *A*, except using three tandemly linked affibodies (SnoopTag–SpyTag–AffiHER2 × 3).

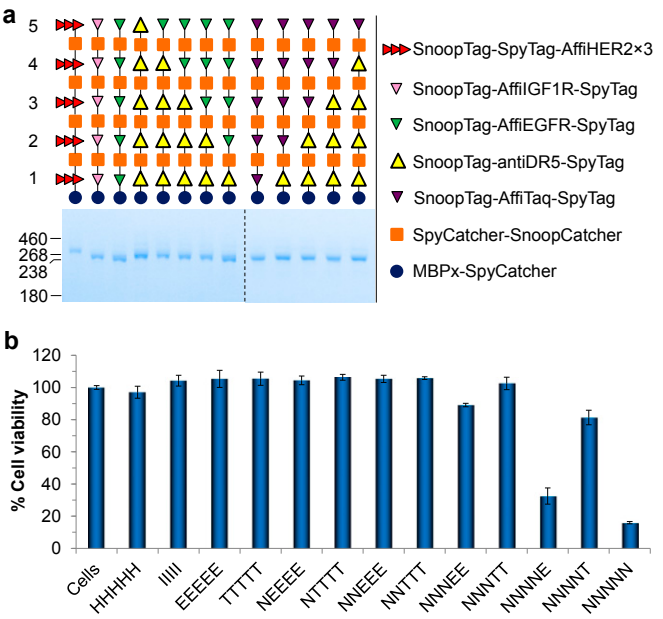

Fig. S7. Effect of valency on polyproteam activation of cell death. (*A*) Synthesis of polyproteam homomultimers or heteromultimers with varying numbers of nanobodies and affibodies to either EGFR or Taq polymerase. Synthesis was analyzed by SDS/PAGE with Coomassie staining. (*B*) Polyproteam effect on viability of MDA–MB-231 after 40 h with each chain, analyzed by a resazurin assay with untreated cells set at 100% (mean ± 1 SD, $n = 3$). E, affibody to EGFR; H, triple affibody to HER2; I, affibody to IGF1R; N, nanobody to DR5; T, affibody to Taq polymerase.